RSC Advances

PAPER

View Article Online
View Journal | View Issue

Cite this: *RSC Adv.*, 2018, **8**, 16013

Preparation of a palygorskite supported KF/CaO catalyst and its application for biodiesel production *via* transesterification

Ya Li * and Yunxia Jiang

This study aimed to explore base catalysts with high transesterification efficiencies to be used for heterogeneous biodiesel production. Palygorskite, a promising low-cost clay mineral, served as a support for KF/CaO to prepare a base catalyst. The base catalyst was prepared *via* a facile impregnation method and characterized using X-ray diffraction (XRD), scanning electron microscopy (SEM) with energy dispersive spectroscopy (EDS), and N_2 adsorption. Subsequently, the prepared catalyst was used for producing biodiesel *via* the transesterification of commercial soybean oil with methanol. The effects of the catalyst preparation conditions as well as the transesterification parameters, such as the loading amount of KF, calcination temperature, catalyst amount, methanol to oil molar ratio, reaction temperature and water content, on the biodiesel yield were investigated. Results showed that the metal oxide species dispersed on the surface of palygorskite, and the formed $KCaF_3$ was the main active component for the activity of the catalyst. A maximum biodiesel yield of 97.9% was obtained under the optimal conditions. The separated catalyst could be directly used in the next round of reactions and gave a satisfactory yield. The biodiesel yields decreased from 97.9% to 91.3% from the first to the tenth use of the catalyst particles.

Received 29th March 2018
Accepted 23rd April 2018

DOI: 10.1039/c8ra02713g

rsc.li/rsc-advances

Introduction

Due to the exhaustion of fossil resources and the increasing emission of pollutants, many studies are now being directed towards the exploitation of alternative renewable fuel.[1] Biodiesel, defined as the monoalkyl esters of fatty acids, has been receiving great attention in recent years as a renewable resource.[2,3] The general method for the preparation of biodiesel is the transesterification reaction of vegetable oil or animal fat with methanol or ethanol in the presence of a catalyst.[4,5] Conventionally, the transesterification has been carried out with homogeneous bases as the catalysts, such as potassium methoxide and potassium hydroxide, because of their high activity.[6–8] However, the use of homogeneous catalysts has many shortcomings, such as the difficulty in product isolation, requirement of large quantities of water, time-consuming nature of the process and environmental pollution from the liquid waste.[9–11]

In order to circumvent the difficulties with homogeneous catalysts, many studies have been conducted in search of ideal solid catalysts which can be separated from liquid products and reused with or without regeneration.[12–14] Recently, some loaded composite catalysts have been developed using supports such as Al_2O_3,[15,16] Fe_3O_4,[17] mesoporous silica,[18,19] cinder[20] and activated carbon.[21,22] Additionally, different kinds of clay, such as zeolite,[23] montmorillonite,[24] kaolin[25] and hydrotalcite,[26] have been employed as heterogeneous catalysts or catalyst supports in biodiesel production. To obtain higher conversion, high temperatures or long reaction times, and even high pressures, were needed for the reaction. Therefore, exploring a high efficiency solid base catalyst that achieves a high biodiesel yield in a short time, has a good tolerance for water, and can be used in heterogeneous biodiesel production is still a challenge. In the present paper, one of our aims was to investigate a solid base catalyst which can catalyze transesterification with a high biodiesel yield at a moderate temperature and with a shorter time. Among the solid catalysts, KF/CaO nanocatalysts showed not only high catalytic ability but also high reusability.[27,28] It was also demonstrated that the formation of $KCaF_3$ was the main reason for the enhancement of catalytic activity.[29–31] This paper aimed to investigate KF/CaO on a natural clay mineral (palygorskite) to prepare solid catalyst particles with high catalytic ability and reusability.

Palygorskite (Pal, formerly called attapulgite, with an ideal formula of $(Mg, Al)_5Si_8O_{20}(OH)_2(H_2O)_4 \cdot 4H_2O$) is a form of crystalline hydrated magnesium aluminum silicate mineral with a unique three-dimensional structure, presenting a fibrous morphology with exchangeable cations and reactive –OH groups on its surface.[32] Palygorskite is widely used as a catalyst carrier because of its unique structure, special adsorptivity and

Nantong College of Science and Technology, Nantong 226007, PR China. E-mail: ly673007@163.com

excellent mechanical resistance. Its natural origin and the low cost make it more attractive.[33,34]

Here, solid base catalysts were prepared by loading KF and CaO on palygorskite (KCa/Pal) *via* an impregnation method and this was characterized using X-ray diffraction (XRD), scanning electron microscopy (SEM) with energy dispersive spectroscopy (EDS), and N_2 adsorption. Subsequently, the prepared catalyst was used for producing biodiesel *via* the transesterification of commercial soybean oil with methanol. The effects of the loading amount of KF, calcination temperature, catalyst amount, methanol to oil molar ratio, reaction temperature and water content on the biodiesel yield were investigated to optimize the transesterification conditions. The reusability and stability of the solid catalyst were evaluated using batch experiments.

Experimental

Preparation of the palygorskite-based KF/CaO catalyst

The clay supported catalyst was prepared *via* a wet impregnation method. 1.0 g CaO and 1.0 g Pal (200 mesh) were immersed in 10 mL KF solution of 0.01–0.05 g mL^{-1}, and this was then magnetically stirred continuously at 25 °C for 3 h and dried at 80 °C for 24 h. After grinding, the resulting product was calcined in a muffle furnace at 300–700 °C for 5 h. The prepared catalyst is denoted KCa/Pal-*m* (m = 10, 20, 30, 40 and 50), where m represents the mass percent of KF for the total amount of Pal and CaO, and Ca/Pal denotes the sample without KF.[35]

Characterization of the as-prepared catalyst

X-ray diffraction (XRD) patterns of the catalysts were obtained using a Rigaku ULTIMA IV diffractometer with high-intensity Cu/Kα radiation and a step scan technique at 2θ angles of 5–90°. The surface morphology of the catalyst was investigated using a JEOL JEM-2100 scanning electron microscope (SEM). Energy dispersive spectroscopy (EDS) was used to conduct the elemental analysis. The Brunauer–Emmett–Teller (BET) method was utilized to measure the specific surface area and pore volume of the catalysts by means of Accelerated Surface Area and Porosity (ASAP 2010, Micromeritics). The pore-size distribution was assessed using the adsorption branch of the isotherm with the Barrett–Joyner–Halenda (BJH) method.

Transesterification reaction

The transesterification reactions were carried out in a 250 mL three-necked flask. The reaction procedure was as follows: first, the soybean oil was added to the flask. Methanol and the catalyst were mixed and then added to the flask. A reflux reaction was performed at the indicated temperature. After that, the catalyst and glycerol were isolated. Methanol was isolated from the biodiesel using a rotary evaporator. The concentrated biodiesel was collected for chromatographic analysis with a heating speed of 10 °C min^{-1}, initial temperature of 160 °C, ultimate temperature of 230 °C, injector temperature of 250 °C and detector temperature of 250 °C.[36] The biodiesel yield was obtained according to the reported method.[37]

Results and discussion

X-ray diffraction of the samples

Fig. 1 depicts the XRD patterns of Pal, Ca/Pal and KCa/Pa-*x* calcined at 500 °C. As shown in Fig. 1a, for Pal, the reflections positioned at 8.3°, 13.9°, 19.9° and 24.5° correspond to crystalline Pal and those at 20.8° and 26.5° are assigned to crystalline quartz.[38] Fig. 1b shows the XRD patterns of Ca/Pal and the diffraction peaks of Pal are still present. The peaks at 17.9°, 29.1°, 36.3°, 47.1° and 54.8° are assigned to the diffraction peaks of $Ca(OH)_2$.[39] The peaks at 32.3°, 37.4° and 53.9° imply that there was the crystal phase of CaO present.[40] Fig. 1c–g show the XRD patterns of KCa/Pa-*x* with different KF load ratios to CaO. Accompanied with the increasing mass ratio of KF, the peaks at 20.7°, 29.0°, 35.1°, 41.2°, 46.7°, 54.8° and 59.5° emerged and were enhanced while the characteristic peaks of $Ca(OH)_2$ and CaO declined. Compared with the standard patterns, the new peaks should belong to the phase of $KCaF_3$.[41] In conclusion, the addition of KF led to the formation of $KCaF_3$, which can improve the activity of the catalyst, and increase the ability to resist the saponification reaction.[42,43] However, when the loading amount of KF was 50 wt%, a diffraction peak at 34.1° corresponding to KF was clearly observed, which may have resulted from excess KF dispersing on the surface of the catalyst.[44]

Surface morphology of the samples

The morphologies of Pal and KCa/Pal-40, characterized using SEM, are shown in Fig. 2. It can be clearly seen from Fig. 2a that Pal exhibits a fibrous structure and some fibers form straight parallel aggregates. The SEM image of KCa/Pal-40 in Fig. 2b is obviously different to that of Pal. After loading CaO and KF, the surface of the KCa/Pal composite was rugged and full of many fragment-like protruding objects. Combined with the results of XRD, the fragments could be ascribed to the crystals of $KCaF_3$. Moreover, the corresponding EDS spectrum of the KCa/Pal-40 composite is displayed in Fig. 2c, showing that the detectable elements include K, Ca and F, indicating that K, Ca and F were successfully deposited on Pal under these synthesis conditions.

N_2 adsorption–desorption

The nitrogen adsorption/desorption isotherms for Pal and KCa/Pal-40 are shown in Fig. 3. Both samples are found to have

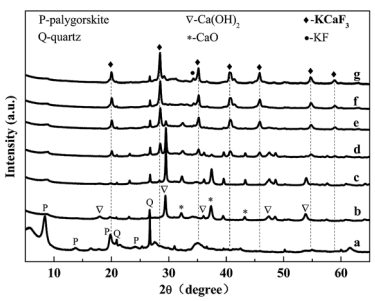

Fig. 1 XRD patterns of Pal (a), Ca/Pal (b), and KCa/Pal-*m* (c–g), where m = 10, 20, 30, 40 and 50, respectively.

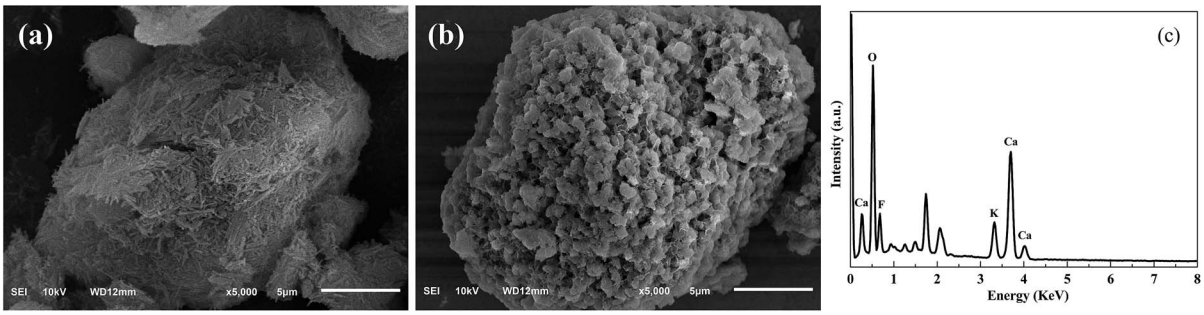

Fig. 2 SEM images of Pal (a) and KCa/Pal-40 (b), and an EDS spectrum of KCa/Pal-40 (c).

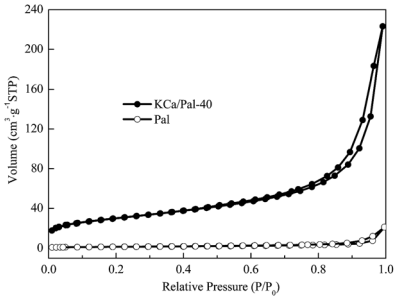

Fig. 3 N_2 adsorption–desorption isotherms of Pal and KCa/Pal-40.

typical IV isotherm curves which contain a hysteresis between the adsorption and desorption curves at relative pressures (P/P_0) ranging from 0.4 to 0.9, suggesting that mesopores exist in Pal and KCa/Pal-40. The BET surface area, pore volume, and average pore size of Pal and KCa/Pal-40 are summarized in Table 1. Pal had a BET surface area of 107.2 $m^2\ g^{-1}$, while after composite formation with KF and CaO, the BET surface area fell to 5.59 $m^2\ g^{-1}$. The pore volumes of Pal and the KCa/Pal-40 composite are 0.34 $m^3\ g^{-1}$ and 0.03 $m^3\ g^{-1}$, respectively. The main pore size distribution centers at 13.47 nm for the Pal sample and 20.37 nm for KCa/Pal-40. The decrease of the specific surface area and pore volume as well as the increase of the average pore size is clearly visible, indicating the clay is successfully covered with the introduced metal oxide species and the micropores are partially blocked.[45] Meanwhile, the large mesopores and surface area of Pal are beneficial to the formation of active sites, providing good catalytic activity for biodiesel synthesis.

Transesterification

Influence of preparation conditions on catalytic activity

To investigate the influence of KF loading on the catalytic activity, a series of catalysts were prepared with different KF loadings (all samples were calcined at 500 °C for 5 h). Table 2 shows the results regarding the effect of KF loading on the catalytic activity. The biodiesel yield is improved from 51.3% to 95.7% when the KF loading increases from 10 wt% to 40 wt%. It can be assumed from these results that the number of active sites on the catalyst surface increases with increasing the loading of KF. When the KF loading is beyond 40 wt%, however, the activity of the catalyst decreased with increased loading of KF, and the biodiesel yield is only 84.3% at 50 wt% KF loading. This is probably due to the fact that the excessive KF covers the active sites of the catalyst surface, resulting in the decrease of catalytic activity.[46] Therefore, the optimum loading of KF is 40 wt% in this study.

Another important parameter to be optimized is the calcination temperature. In the preparation process for the catalyst, calcination treatment of the catalyst at a high temperature is favorable for the interaction between the support and active ingredient, which generates new active sites for the catalyst. Therefore, the calcination temperature is crucial for increasing the catalytic activity. Fig. 4 shows the results concerning the influence of the calcination temperature on the catalytic activity of KCa/Pal-40. Clearly, the biodiesel yield initially increases with the increase of calcination temperature. Then, the yield reaches a maximum value at a calcination temperature of 500 °C. However, the biodiesel yield decreases gradually with further increase of the calcination temperature. This is probably due to the fact that overheating results in surface sintering and a reduction of the specific surface area, which in turn leads to a decrease in the catalytic activity.[42] The current results indicate that the optimal calcination temperature is 500 °C.

Influence of reaction parameters on the biodiesel yield

The effect of the molar ratio of methanol to soybean oil on the transesterification was investigated. As illustrated in Fig. 5, with an increase in the methanol/oil molar ratio, the biodiesel yield increased rapidly and reached a high value at a methanol/oil molar ratio of 12 : 1. When the methanol/oil molar ratio was more than 12 : 1, the increase of the biodiesel yield was not significant. Therefore, to guarantee the biodiesel quality, the optimal methanol/oil molar ratio of 12 : 1 was selected for the further research.

Table 1 Physical properties of Pal and KCa/Pal-40

Sample	BET surface area ($m^2\ g^{-1}$)	Total pore volume ($m^3\ g^{-1}$)	Average pore size (nm)
Pal	107.2	0.34	13.47
KCa/Pal-40	5.59	0.03	20.37

Table 2 Effect of the mass percent of KF on the biodiesel yield[a]

Catalyst	Basicity (mmol g^{-1})	Biodiesel (%)
KCa/Pal-10	0.34	51.3
KCa/Pal-20	0.41	78.2
KCa/Pal-30	0.57	84.5
KCa/Pal-40	0.71	95.7
KCa/Pal-50	0.62	82.1

[a] Transesterification conditions: a molar ratio of methanol to oil of 12 : 1, the catalyst 3 wt% of the oil, a temperature of 65 °C, a reaction time of 2.5 h and the water 2.5 wt% of the oil.

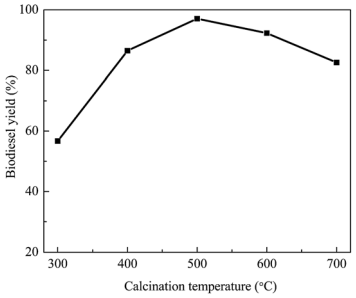

Fig. 4 Effect of calcination temperature on biodiesel yield. Transesterification conditions: a molar ratio of methanol to oil of 12 : 1, the catalyst 3 wt% of the oil, a temperature of 65 °C, a reaction time of 2.5 h and the water 2.5 wt% of the oil.

The usage of the catalyst can be beneficial to obtain a high product yield in a relatively short reaction time. However, an excessive amount of catalyst leads to an increase of the viscosity of the reaction system and causes a problem with mixing as well as a demand for higher power consumption for adequate stirring. To overcome this kind of problem, the appropriate amount of catalyst had to be investigated. As shown in Fig. 6, the biodiesel yield was greatly increased by increasing the amount of catalyst from 1 to 3 wt% by weight of oil. However, as the catalyst dosage was continuously increased, the biodiesel yield improved slightly. This means that an excess amount of catalyst could not further promote the yield because the reaction had reached equilibrium. So, the amount of catalyst was chosen to be 3 wt% by weight of oil for our studies.

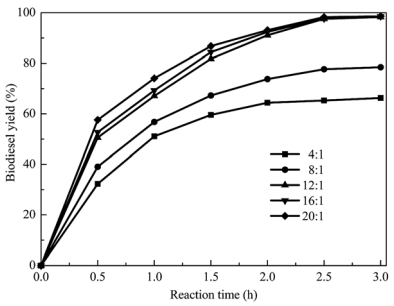

Fig. 5 Effect of molar ratio of methanol to soybean oil. Transesterification conditions: the catalyst 3 wt% of the oil, a temperature of 65 °C, a reaction time of 2.5 h and the water 2.5 wt% of the oil.

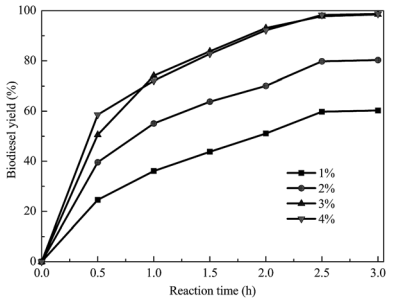

Fig. 6 Effect of catalyst usage on biodiesel yield. Transesterification conditions: a molar ratio of methanol to oil of 12 : 1, a temperature of 65 °C, a reaction time of 2.5 h and the water 2.5 wt% of the oil.

In addition, the effect of temperature on biodiesel yield was examined. Fig. 7 shows that the biodiesel yield significantly increased from 50 °C to 65 °C. From Fig. 7, it can be seen that the biodiesel yield significantly increased from 50 °C to 65 °C, and the highest yield was at 65 °C. However, the yield decreased when the temperature was higher than 65 °C. This is mainly because the evaporation of methanol reduces the contact time between methanol and oil, resulting in a lower biodiesel yield.[47]

In the transesterification of soybean oil to biodiesel catalyzed by a solid base, the biodiesel yield is greatly affected by water. Fig. 8 shows the application of soybean oils containing various amounts of water for biodiesel synthesis catalyzed by KCa/Pal-40. The yield of biodiesel is increased from 89.3% to 97.9% when the water content increases from 0 to 2.5 wt% of soybean oil. This is probably due to the fact that water molecules are adsorbed first on the surface of the catalyst to form OH^-. Then, the surface OH^- abstracts a proton from methanol to generate CH_3O^-. Certainly, the catalyst can also abstract H^+ from methanol to form CH_3O^-. But OH^- is more easily adsorbed on the catalyst surface than CH_3O^-.[37] When the water content is beyond 2.5 wt%, the biodiesel yield decreases with the increase of water content. Therefore, the water content in oil should be kept under 2.5 wt% to prevent catalyst deterioration and biodiesel hydrolysis.

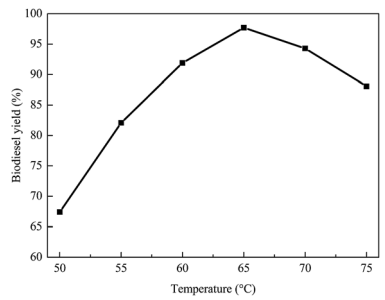

Fig. 7 Effect of reaction temperature on biodiesel yield. Transesterification conditions: a molar ratio of methanol to oil of 12 : 1, the catalyst 3 wt% of the oil, a reaction time of 2.5 h and the water 2.5 wt% of the oil.

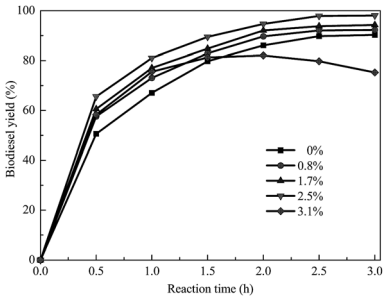

Fig. 8 Effect of water content on biodiesel yield. Transesterification conditions: a molar ratio of methanol to oil of 12 : 1, the catalyst 3 wt% of the oil, a temperature of 65 °C and a reaction time of 2.5 h.

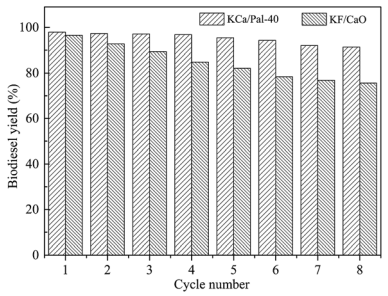

Fig. 9 Reusability and recovery of KCa/Pal-40 and KF/CaO. Transesterification conditions: a molar ratio of methanol to oil of 12 : 1, the catalyst 3 wt% of the oil, a temperature of 65 °C, a reaction time of 2.5 h and the water 2.5 wt% of the oil.

Reusability of the catalyst

From an economic point of view, the reusability of the catalyst is of great importance for industrial applications. After the reaction had completed, the catalyst was separated from the reaction mixture using only simple centrifugation or filtration to investigate its lifetime and stability. Prior to each reaction, the same amount of fresh commercial soybean oil and methanol were added, and the same reaction conditions were used. Fig. 9 shows the effect of repeated use of the KCa/Pal-40 and KF/CaO catalysts on the transesterification reaction. It is found that the biodiesel yield for the reaction catalyzed with KF/CaO was 75.6% after 10 cycles of reuse. However, the KCa/Pal-40 catalyzed synthesis of biodiesel still produced a yield in excess of 91.3% after being reused for the same number of times. Therefore, KCa/Pal-40 can contribute much to decreasing the cost of biodiesel production due to its long catalyst lifetime and short reaction time.

Conclusion

In the present work, a solid basic catalyst, KCa/Pal, was used to catalyze the transesterification of soybean oil with methanol to produce biodiesel. It is demonstrated that the KCa/Pal catalyst exhibits high catalytic activity in the transesterification reaction. When the reaction was carried out under reflux with methanol, with a molar ratio of methanol to soybean oil of 12 : 1, the biodiesel yield catalyzed by 3% catalyst (based on the weight of soybean oil) reached 97.9% in 2.5 h at 65 °C. The catalyst is promising for use in the continuous production of biodiesel. According to the results of catalyst characterization, the formed $KCaF_3$ should be the main active component for the catalytic activity. Meanwhile, the catalyst exhibited relatively good reusability. The biodiesel yield remained at 91.3% over the 10 times the catalyst was used.

Conflicts of interest

There are no conflicts to declare.

Acknowledgements

We acknowledge the support of the Scientific Research Foundation for Doctoral Teachers of Nantong College of Science and Technology (NTKY-Dr2015002) and Qing Lan Project of Jiangsu Province (2017).

Notes and references

1 C. C. C. M. Silva, N. F. P. Ribeiro, M. M. V. M. Souza and D. A. G. Aranda, *Fuel Process. Technol.*, 2010, **2**, 205–210.
2 A. Datta and B. K. Mandal, *Renew. Sustain. Energy Rev.*, 2016, **57**, 799–821.
3 Y. C. Sharma, B. Singh and S. N. Upadhyay, *Fuel*, 2008, **12**, 2355–2373.
4 S. T. Keera, S. M. E. Sabagh and A. R. Taman, *Fuel*, 2011, **1**, 42–47.
5 E. Anderson, M. Addy, Q. Xie, H. Ma, Y. Liu and Y. Cheng, *Bioresour. Technol.*, 2016, **200**, 153–160.
6 K. G. Georgogianni, A. K. Katsoulidis, P. J. Pomonis, G. Manos and M. G. Kontominas, *Fuel Process. Technol.*, 2009, **7–8**, 1016–1022.
7 M. Agarwal, G. Chauhan, S. P. Chaurasia and K. Singh, *J. Taiwan Inst. Chem. Eng.*, 2012, **1**, 89–94.
8 A. Aliyu, E. Lomsahaka and A. Hamza, *Adv. Appl. Sci. Res.*, 2012, **1**, 615–618.
9 J. Zhang, S. Chen, Y. Rui and Y. Yan, *Fuel*, 2010, **10**, 2939–2944.
10 M. Kouzu and J. S. Hidaka, *Fuel*, 2012, **1**, 1–12.
11 L. Cui, G. Xiao, X. Bo and G. Teng, *Energy Fuels*, 2007, **6**, 3740–3743.
12 W. Li, D. Ma, S. Yao, Y. Gao and N. Yan, *Green Chem.*, 2015, **17**(15), 4198–4205.
13 K. Sun, A. R. Wilson, S. T. Thompson and H. H. Lamb, *ACS Catal.*, 2015, **5**(16), 1939–1948.
14 J. A. Botas, D. P. Serrano, A. García and R. Ramos, *Appl. Catal., B*, 2014, **145**, 205–215.
15 Y. Tang, H. Ren, F. Chang, X. Gu and J. Zhang, *RSC Adv.*, 2017, **10**, 5694–5700.
16 D. M. Marinkovic, J. M. Avranović, M. V. Stanković, O. S. Stamenković, D. M. Jovanović and V. B. Veljković, *Energy Convers. Manage.*, 2017, **144**, 399–413.
17 A. M. Tamilmagan and A. G. Priyabijesh, *Int. J. ChemTech Res.*, 2015, **5**, 90–96.

18 Y. Chen, J. Han and H. Zhang, *Appl. Surf. Sci.*, 2008, **18**, 5967–5974.
19 C. Samart, C. Chaiya and P. Reubroycharoen, *Energy Convers. Manage.*, 2010, **7**, 1428–1431.
20 H. Liu, L. Su, F. Liu, C. Li and U. U. Solomon, *Appl. Catal., B*, 2011, **3**, 550–558.
21 A. Buasri, B. Ksapabutr, M. Panapoy and N. Chaiyut, *Korean J. Chem. Eng.*, 2012, **12**, 1708–1712.
22 S. Baroutian, M. K. Aroua, A. A. Raman and N. M. Sulaiman, *Bioresour. Technol.*, 2011, **2**, 1095–1102.
23 H. Wu, J. Zhang, Q. Wei, J. Zheng and J. Zhang, *Fuel Process. Technol.*, 2013, **9**, 13–18.
24 M. A. F. Othman, *BMC Cell Biol.*, 2015, **6**, 759.
25 T. H. Dang, B. H. Chen and L. Duujong, *Bioresour. Technol.*, 2013, **4**, 175–181.
26 G. Lee, Y. K. Ji, Y. Ning, Y. W. Suh and C. J. Ji, *J. Mol. Catal. A: Chem.*, 2016, **423**(27), 347–355.
27 W. Yun, S. Y. Hu, Y. P. Guan, L. B. Wen and H. Y. Han, *Catal. Lett.*, 2009, **3–4**, 574–578.
28 S. Hu, L. Wen, Y. Wang, X. Zheng and H. Han, *Bioresour. Technol.*, 2012, **3**, 413–418.
29 L. Gao, G. Teng, G. Xiao and R. Wei, *Biomass Bioenergy*, 2010, **9**, 1283–1288.
30 H. Liu, L. Su, Y. Shao and L. Zou, *Fuel*, 2012, **7**, 651–657.
31 J. Chen, L. Jia, X. Guo, L. Xiang and S. Lou, *RSC Adv.*, 2014, **104**, 60025–60033.
32 Y. Li, J. C. Hu and P. F. Han, *Chin. J. Chem. Eng.*, 2015, **5**, 822–826.
33 A. Xue, S. Zhou, Y. Zhao, X. Lu and P. Han, *J. Hazard. Mater.*, 2011, **5**, 7–14.
34 J. Huang, Y. Liu and X. Wang, *J. Mol. Catal. B: Enzym.*, 2009, **1**, 10–15.
35 L. Jia, Y. Li, J. Chen, X. Guo, S. Lou and H. Duan, *Res. Chem. Intermed.*, 2015, **3**, 1–17.
36 X. Chen, W. W. Qian, X. P. Lu and P. F. Han, *Nat. Prod. Res.*, 2012, **13**, 1249–1256.
37 X. Liu, H. He, Y. Wang, S. Zhu and X. Piao, *Fuel*, 2008, **2**, 216–221.
38 K. C. M. Xavier, M. D. S. F. D. Santos, M. R. M. C. Santos, M. E. R. Oliveira, M. W. N. C. Carvalho, J. A. Osajima, E. C. D. Silva Filho, J. A. Osajima and E. C. D. Silva Filho, *Mater. Res.*, 2014, **8**, 3–8.
39 N. Asikin Mijan, H. V. Lee and Y. H. Taufiq Yap, *Chem. Eng. Res. Des.*, 2015, **102**, 368–377.
40 G. Moradi, M. Mohadesi and Z. Hojabri, *React. Kinet. Mech. Catal.*, 2014, **1**, 169–186.
41 M. Kaur and A. Ali, *Eur. J. Lipid Sci. Technol.*, 2014, **1**, 80–88.
42 S. Hu, Y. Guan, Y. Wang and H. Han, *Appl. Energy*, 2011, **8**, 2685–2690.
43 M. Kouzu, T. Kasuno, M. Tajika, Y. Sugimoto, S. Yamanaka and J. Hidaka, *Fuel*, 2008, **12**, 2798–2806.
44 L. Gao, X. Bo, G. Xiao and J. Lv, *Energy Fuels*, 2008, **5**, 3531–3535.
45 J. J. Li, Z. Mu, X. Y. Xu, H. Tian, M. H. Duan and L. D. Li, *Microporous Mesoporous Mater.*, 2008, **1**, 214–221.
46 C. Sun, F. Qiu, D. Yang and B. Ye, *Fuel Process. Technol.*, 2011, **126**, 383–391.
47 L. Wen, Y. Wang, D. Lu, S. Hu and H. Han, *Fuel*, 2010, **9**, 2267–2271.